CLINICOPATHOLOGICAL CASE

Burkitt's lymphoma with medullary cavity infiltration. Case report

Luis Enrique Juárez Villegas, Stanislaw Sadowinski-Pine, Daniel Ibarra-Ríos, and Mariana Sánchez-Curiel Loyo

Case report

We present the case of a 46-month-old female who was referred to our institution from a secondary-care hospital due to difficulty walking, anuria, palpebral edema, upper and lower limb edema and abdominal distension. The patient was the product of a first pregnancy of a 24-year-old mother who smoked during the first pregnancy trimester but was otherwise healthy. The patient's father was a 25-year-old rural dweller with weekly alcohol consumption (until inebriation) for the past 10 years and a smoker for the last 8 years (10 cigarretes daily); he was otherwise healthy. The family is native to and continues to live in Ignacio Zaragoza, Durango (Mexico). They live in their own house with all basic urban services. The patient was fed with formula from birth until she was 6 months old when she then received fruits and vegetables and began eating the normal family diet when she reached 2 years of age. She presented appropriate psychomotor development and vaccination scheme.

Symptom onset

The patient presented difficulty walking and experienced falls for 20 days. Three days later she presented anuria, palpebral edema, upper and lower limb edema and abdominal distension. She was treated at a secondary-care hospital where they administered dialysis and transfusion of packed red cells.

Physical examination

The patient presented generalized skin and tegument pallor and lower lip ecchymosis. She was well hydrated. Somatometry and vital signs were as follows: weight (16 kg), height (100 cm), heart rate (140 beats/min), respiratory frequency (26 breaths/min), blood pressure (110/60 mmHg), and temperature (36.5 °C). She was normocephalic with equal, round pupils reactive to light. Auditory canals were permeable with complete tympanic membranes. Dental caries were apparent in second molars, pharynx was without hyperemia and discharge, neck was cylindrical without adenomegalies, and jugular plethora was present. Cardiac sounds were rhythmic with some tachycardia. Lung fields were clear with appropriate air exchange and no added phenomena. Abdomen was soft, depressible and distended with placement of a soft Tenchkoff catheter. Condition of the surrounding skin was inappropriate, presenting leakage from dialysis fluid. The patient presented with phenotypic female genitalia. Limbs demonstrated appropriate capillary filling without edema and range of motion was preserved. The patient presented weakness and limited sensitivity in lower limbs as well as loss of equilibrium.

[1]Departamento de Patología, Hospital Infantil de México Federico Gómez, México, D.F., México.

Received for publication: 12-8-09
Accepted for publication: 01-12-10

The Neurology Department reports this as a profile compatible with lower motor neuron polyneuropathy associated with hyperazotemia. Somatosensory-evoked potentials and nerve conduction velocity tests were requested. The patient was managed with a soft, low-sodium diet, 400 mL/m^2/SC/day total liquids, 0.7 mg/kg/day omeprazole, and peritoneal dialysis was administered using 500 mL 4.25% hypertonic solution for 30 min in the abdominal cavity. Three days later, polyvitamins were added (1 tablet/24 h), 5 mg/24 h folic acid, and 500 mg/8 h calcium carbonate. Peritoneal dialysis was initiated (30 mL/kg) using 1.5% standard solution for 45 min.

Evolution

During the following days, the patient presented water-electrolyte imbalance, metabolic imbalance, dehydration, hypotension and metabolic acidosis. Tenchkoff catheter is removed because of malfunction and replaced by a Mahurkar catheter for hemodialysis.

Nine days after admission, magnetic resonance of the spine was carried out, revealing a homogeneous, isointense mass in T1 and T2 extending from vertebral body L1 to L4, penetrating towards the intervertebral foramen contacting and displacing the spinal cord and nerve roots. Oncology Department suggests that this may be a case of Burkitt's lymphoma. An urgent tumor biopsy was suggested because of compression of the cauda equina. Bone marrow aspiration was reported as normal. Tru-cut right renal biopsy was carried out. This oncological urgency triggers empiric chemotherapy using 300 mg/m^2/SC/day cyclophosphamide and 1 mg/m^2/SC/day dexamethasone.

The patient presented seizures that receded spontaneously. Afterwards, irritability, cyanosis and neurological deterioration were observed so the patient was intubated. The patient was referred to the Pediatric Intensive Care Unit (PICU) where she presented 40/30 mm Hg hypotension, tachycardia, pallor and dissociated ventilatory response; therefore, hemodialysis was suspended. When placing the catheter into the right internal jugular the guide was accidentally lost. Its extraction was impossible and it remained in the internal jugular as well as in the superior vena cava and right atrium. On the following day, the catheter was removed without complications. The patient presents fever and was managed with vancomycin and cefotaxime. She presented cardiopulmonary arrest for 6 min and responded after three resuscitation cycles and three doses of adrenalin; hemodialysis was suspended.

Because of fever, the patient was managed with 150 mg/kg/day cefepime and 15 mg/kg/day amikacin. Renal biopsy report is compatible with B-cell lymphoblastic non-Hodgkin's lymphoma. Patient presented elevation of pancreatic enzymes and persistant uric acid elevation up to 22.6 mg/dL. Creatinine was 2.0 mg/dL with 132 mEq/L sodium, 3.0 mEq/L potassium, 5887 U/L lactate dehydrogenase (LDH), 338 U TGO, 147 U TPG, and 1.0 g/dL albumin. Hemoculture was positive to yeasts and *Candida*. The central venous catheter was removed and the patient was administered amphotericin (1 mg/kg/day). Chest X-ray revealed full right atelectasis. Chemotherapy was restarted due to disease progression using 1 mg vincristine, 500 mg cyclophosphamide, 30 mg adriamycin and 8 mg dexamethasone per day. Trimethroprim and sulfamethoxazole were added after positive immunofluorescence to *Pneumocystis jirovecii*. Laryngoscopy is carried out through cannula, revealing erythematous longitudinal lesions that bled easily and a large amount of thick mucus in the left inferior bronchus. *Candida tropicalis* was isolated from the central venous catheter, thus continuing therapy with 1.5 mg/kg/day amphotericin. Meropenem was added (100 mg/kg/day) because of deep neutropenia and risk of infection from multiresistant nosocomial germs. A new computed tomography revealed renal images compatible with microabscesses. Tubes were removed without tolerance, so patient was reintubated on the same day (July 21). Mahurkar catheter was removed and a new central venous catheter was placed.

Real-time polymerase chain reaction was positive for Epstein-Barr virus (EBV) with 1 070 copies

in peripheral blood and 472 in plasma. Tubes were removed and patient received ventilatory support using BPAP. Gammaglobulin was added (400 mg/kg/day) every 48 h. Infectology Service reduced amphotericin dosage (1 mg/kg/day) discarding aspergillosis, based on X-ray evidence. At that time, creatinine was 2.1 mg/dL with 133 mEq/L sodium, 3.6 mEq/L K, 88 mEq/L Cl and 8.6 mg/dL Ca. Blood tests revealed Hb (8.9 g/dL), leukocytes (200/mm^3), and platelets (33,000). LDH decreased to 342 U/L as well as 10 U/L TGO and 22 U/L TPG. *C. tropicalis* cultures continued to be positive in the central venous catheter, peripheral catheter and Mahurkar catheter; therefore, they were removed. Hemodialysis sessions were suspended as well as amphotericin-B, changing antifungal treatment to caspofungin (70 mg/m^2/SC/day). Furosemide was added to force diuresis. Assisted ventilation was restarted because of deterioration of ventilatory function. A Mahurkar catheter was placed in the right saphenous vein and hemodialysis was restarted 3 days after previous schema. Dobutamine infusion was administered at the PICU (5 μg/kg/min) and 0.1 μg/kg/min norepinephrine because of hypotension at an average of 35 mm Hg. Ventilatory parameters were increased because of 47% oxemia and a left jugular catheter was again placed in order to have a new central access. Patient was placed in a prone position for alveolar recruitment, which improves oxemia, and amines were suspended. Hypoxemia gasometry persisted, requiring high PEEP, high frequencies and respiratory acidosis. Patient was then managed with high-frequency oscillatory ventilation with FIO_2 60%, maximum inspiratory pressure (MIP) 19, positive end-expiratory pressure (PEEP) 28, (spell out IT) 33. Echocardiogram was carried out with 70% ejection fraction (EF), finding a 6 x 3 mm diameter refractive image in right ventricle, suggesting endocarditis.

After 49 days of hospital stay, the patient presented hypothermia for 7 h and bradycardia that evolved to cardiorespiratory arrest without response to advanced resuscitation maneuvers that were applied for min. The patient was managed with hemodialysis every 24-48h during her stay and was anuric up to 2 days before her death.

Radiological findings

Dr. Mariana Sánchez Curiel Loyo

This patient has an extensive radiological file. We present the most relevant images for the disease. On June 23 we requested a renal ultrasound. Increase in the size of both kidneys was remarkable: 12 cm on longitudinal axis and 7 cm on anteroposterior axis (Fig. 1) as well as bilateral hypoechogenicity when compared to adjacent liver and corticomedullary relationship loss. The bladder was distended, which limits its evaluation. Renal arteries spectra were requested. Resistance indexes were mildly elevated for patient's age and there are data compatible with diffuse renal damage from undetermined etiology. On June 30 magnetic resonance imaging studies of thorax and lumbar region revealed increased size of kidneys with some mixed areas with higher and lower signal intensity in T1 and T2 sequences (Fig. 2) as well as right paravertebral mass (Fig. 3). There were changes in signal intensity from bone trabecula and vertebral bodies, mainly in L2 and L4. We identified a round mass in the pelvic cavity observed in both sequences with heterointense contents. A paravertebral mass extended through L2 and L3 foramina toward the medullary cavity, compressing the sac and displacing it laterally. The mass equaled the size of four vertebral bodies. At the age of this patient, vertebral bodies measure between 1 and 1.5 cm in height. Paravertebral mass was 2-2.5 vertebral bodies (Fig. 4). This mass was isointense when compared to psoas muscle, which was laterally displaced. Increase in kidneys size persisted in both sequences. On July 7 we carried out a chest and abdominal tomography with endovenous contrast and for pulmonary parenchyma. On pulmonary window, it is worth noticing a mixed pulmonary pattern characterized by a nodular infiltrate distributed on the base of the left lung and another bronchoalveolar infiltrate better identified as the mediastinum with scarce air bronchogram predom-

inantly on the left. There was ipsilateral pleural thickening. Mediastinum presented no adenopathies. Both kidneys still presented an increased size. Hyperdense images were observed and may be related to calcification. There was perisplenic fluid. Tomography done on July 23 revealed a persistent nodular pattern extending toward the right lung. There are unpolished glass images at bases toward the posterior segments and one on the right apex. Liver size was increased, measuring 20 cm with free surrounding fluid and heterogeneous posterior endovenous contrast uptake charaterized by nodular images. We identified an area of periportal hypodensity, possibly related to periportal edema and free fluid on pelvic cavity. The last CT revealed a chronically damaged lung pattern with destruction characterized by mixed interstitial broncoalveolar pattern

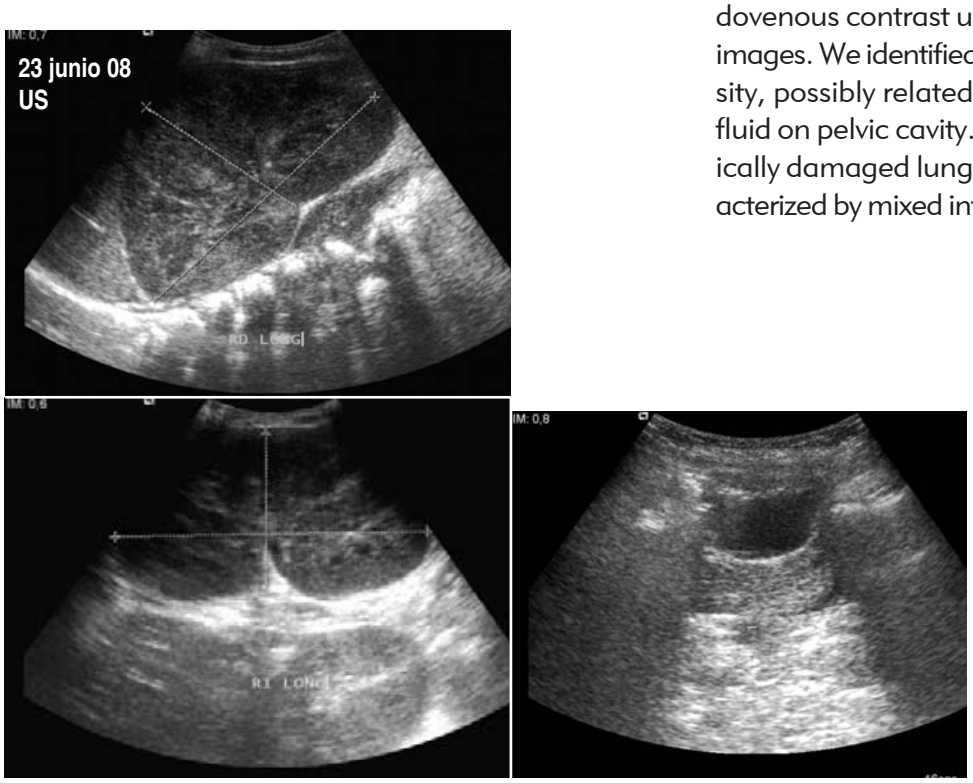

Figure 1. Renal ultrasound showing increased size of both kidneys.

Figure 2. Magnetic resonance showing increased size of both kidneys with heterointense images within.

(Fig. 5). There was persistent hepatomegaly with pelvic fluid with the aforementioned mass. Final radiological diagnoses were bilateral thickening and pleural effusion, multiple-foci bilateral pneumonia progressing to bilateral symmetrical occupation possibly associated with hemorrhage, bilateral nephromegaly probably secondary to infiltration process, right paravertebral and intraspinal process involving vertebral bodies L2-L4, free fluid in abdominopelvic cavity, and a mass in the pelvic cavity with undetermined etiology.

Clinical case discussion

Dr. Daniel Ibarra Rios

The 46-month-old patient was a native of Ignacio Zaragoza, Durango, public land founded on February 4, 1929 by Plutarco Elias Calles. It has 3047 inhabitants dedicated to cattle and poultry farming. Tele-education systems were founded in 1984 and 1996 for junior-high and high-school, respectively. Electricity supply was completed in 1998.[1] The State Oncology Center of Durango currently has 132 pediatric cancer cases. Of these patients, 50% have

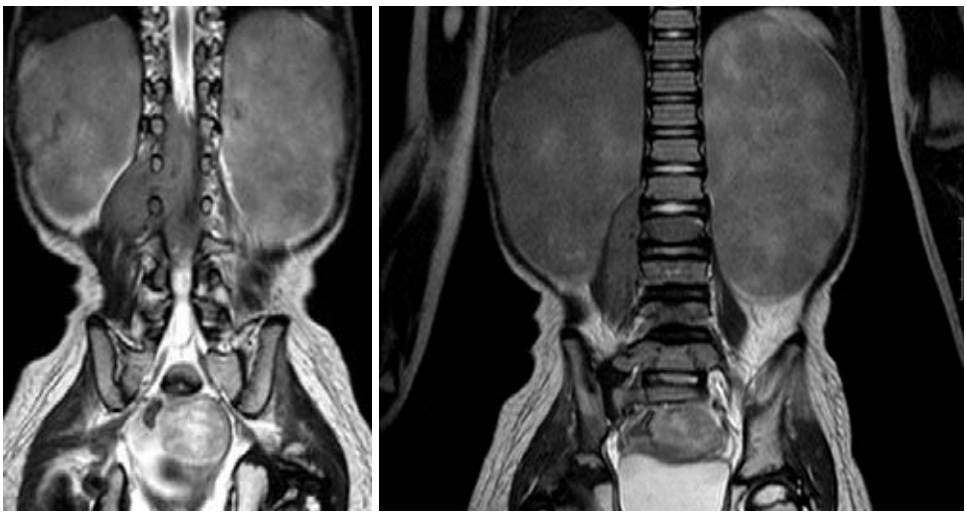

Figure 3. Magnetic resonance showing right paravertebral tumor.

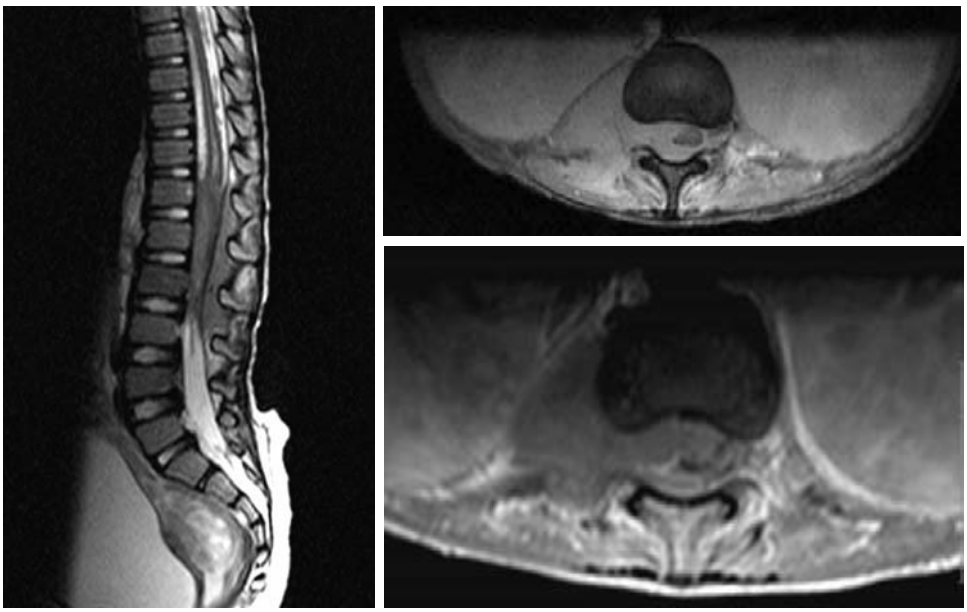

Figure 4. Magnetic resonance showing right paravertebral tumor extending through intervertebral foramina.

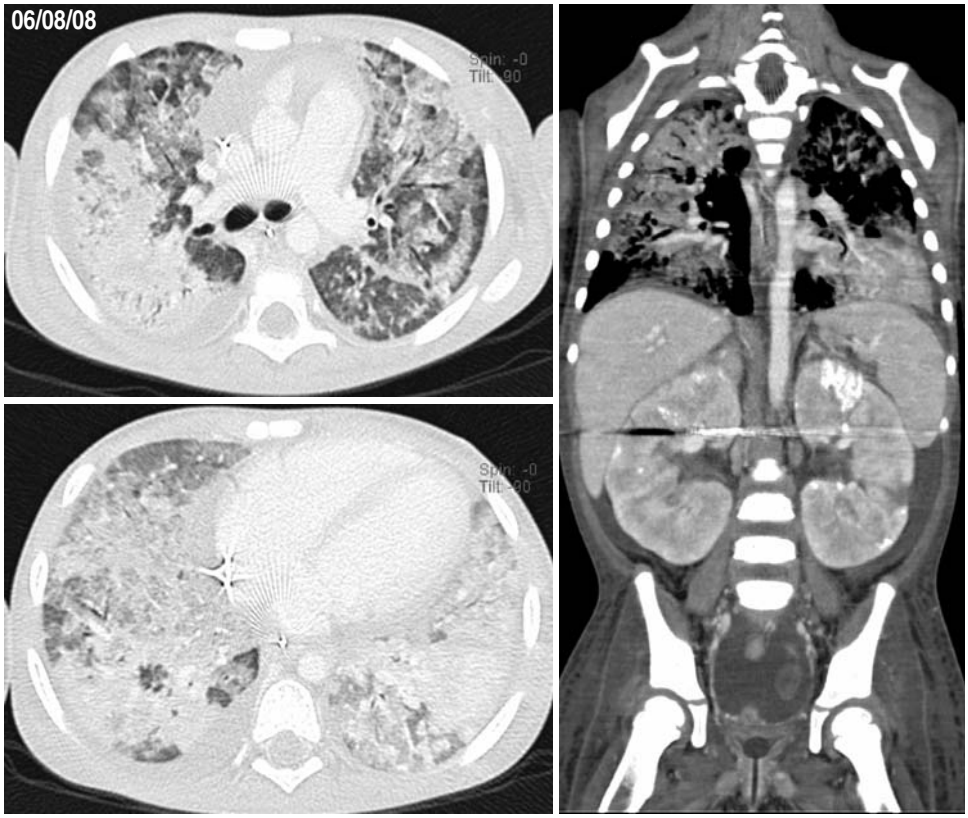

Figure 5. Computed tomography of the chest showing pulmonary pattern with chronic destructive damage.

leukemia, 30% are native of central Durango, 20% are from Zacatecas and 50% are from rural Durango.

The patient was exposed to tobacco smoke because both parents smoked. Tobacco smoke contains 4 000 compounds and, of these, 60 are confirmed or suspected carcinogens. Many studies have associated in utero and postnatal exposure to tobacco smoke with leukemia and lymphoma. Although results are inconsistent, mutagenicity and genotoxicity caused by transplacental exposure to tobacco smoke has been well documented.[2,3] The patient was born at pregnancy term with a weight of 4 kg. Because of family history, the mother should have been assessed for diabetes. The patient presented meconium aspiration syndrome and aspiration syndrome so she remained for 15 days at the hospital. This may have increased the risks of pulmonary hypertension and subclinical residual pulmonary problems that may have contributed to ventilatory outcome during her hospital stay.

Because the patient lived in a rural environment, it is possible that she was exposed to pesticides.[4] There are studies with statistically significant results that relate pesticide exposure with lymphoma. Flower et al.[5] reported a standardized incidence of 1.36, meaning 1.36 cases beyond expected are observed when patients have pesticide exposure. Ma and Buffler reported a relationship with leukemia, finding an odds ratio of 2.8. The risk was higher when there was in-house exposure during pregnancy.[6]

The patient presented normal psychomotor development. She had a complete vaccination scheme according to 1999 recommendations. In 2004, the national vaccination scheme added influenza A and in 2007 added rotavirus and pneumococcus vaccinations with reinforcement for five vaccinations at 18 months.

At some point the patient had contact with EBV as shown by PCR amplification. An antigenic test

would be required to determine the time she was exposed. Seroepidemiological studies have demonstrated that this virus has a high prevalence, usually causing subclinical disease in children. Depending on the studied population, infection rate varies between 20 and 80% at 3 years of age. After a primary infection, this virus latently infects B-cell lymphocytes, spreading to saliva and genital secretions. Virus dissemination has been associated with low socioeconomic status, overcrowding and poor hygiene. When at rest in peripheral blood B-cells, the virus remains virtually invisible to the immune system because it expresses few viral proteins. *In vitro* B-cell infection caused by this virus results in cell immortality and expression of several activation and adhesion molecules. There are at least 11 genes in the viral genome associated with replication, such as EBNA1, B-cell activation such as LMP-1 and cell-cycle progression such as ABNA-2.[7]

Therefore, lymphocyte proliferation took place and produced two oncological urgencies that may explain the current disease physiopathology. First, a tumor lysis syndrome (TLS) produced acute renal insufficiency (ARI) in a previously infiltrated kidney and second, there was medullary compression (also from infiltration) producing the lower motor neuron syndrome diagnosed at admission.

Prior to admission to our institution, the patient had been treated at a secondary-care hospital where she was admitted for ARI. In order to correct metabolic alterations, a dialysis process was started and she received packed red cells. At admission she was eutrophic with 100% weight and size for age, considering the extra weight from dialysis when she was weighed. The following discussion will be presented in three parts considering renal pathology, neoplasm and infectious complications.

Renal pathology

It is possible that the patient presented nephrotic syndrome secondary to infiltration.[8] Glomerular damage associated with neoplasms has been well documented in the medical literature; however, actual pediatric prevalence is unknown because several patients with minor urinary alterations are seldom subjected to invasive study. Renal insufficiency may generate protein loss per se and produce a physiopathology similar to nephrotic syndrome.

The patient also presented TLS that accelerated ARI. Upon admission, the patient scored 11.7 according to the Schwartz scale for renal insufficiency. She also presented hyperuricemia, hyperkalemia and hyperphosphatemia that, although these were noncompliant with American Oncology Association parameters, we should consider there was a previous dialysis process. TLS is described as a group of biochemical alterations associated with rapid cellular destruction. The cancer types most frequently associated are non-Hodgkin's lymphomas and leukemias. A Nigerian study (1994-2003) including 123 children with ARI reported that 29% of cases had primary etiologies and of these, 47.2% were Burkitt's lymphoma.[9] Peritoneal dialysis continues, biochemical parameters improve and metabolic acidosis is compensated. On June 29 a Mahurkar catheter was placed, carrying out hemodialysis every 24-48 h with hyperuricemia and hyperphosphatemia as key markers. Renal function finally improved, and the latest Schwartz evaluation was 34.3. Dialysis was an appropriate management although hemodialysis is preferred because metabolic alterations can be corrected more quickly. It has been suggested, even as prophylactic treatment, to subject patients with Burkitt's lymphoma to continuous venous hemodiafiltration before starting chemotherapy. Early recognition of tumor lysis and renal insufficiency is key. Recommended management includes hyperhydration, urinary alkalization, and specific control of potassium, phosphorus and uric acid with allopurinol.[10] The current recommendation is still to begin dialysis early before refractory hyperkalemia, hyperphosphatemia >10 mg/dL, uric acid >10 mg/dL, hypervolemia, uremic syndrome, metabolic acidosis and hourly diuresis <100 mL/m^2/SC in spite of hyperhydration. Additional challenges to keep in mind are that sepsis reduces blood flow and maintaining renal insufficiency reduces circulating volume. There are also direct

effects from endotoxins and exotoxins such as tumor necrosis factor, several cytokines, and nitric oxide pathway dysfunction.[11] *Candida* infection can affect all structures including glomeruli, tubules, collecting systems, ureters and bladder. Microabscesses can form on renal parenchyma and obstruction may be found at any level.

Neoplasm

The term "leukemia" is used to describe lymphoid neoplasms that involve bone marrow generally accompanied by a large number of tumor cells in peripheral blood. On the other hand, the term "lymphoma" is used to describe proliferations from tissue masses. Sometimes the difference between lymphoblastic leukemia and lymphoma is unclear and, frequently, only the histological distribution is described during diagnosis. The World Health Organization (WHO) classifies lymphoid neoplasms according to five broad categories: immature B-cells, mature B-cells, immature T-cells, mature T-cells and natural killer cells and Hodgkin's lymphoma.[12] Leukemia represents the most frequent neoplasm during childhood in Mexico with a prevalence between 30 and 34% of new cases.

Of these cases, 80% are acute lymphoblastic leukemia. Lymphomas account for 10-15% of all pediatric cancers with an annual incidence of 1-2.6 cases per million. The age range varies from 3 years to adolescence with an average onset at 7 years of age. Non-Hodgkin's lymphomas are a group of diseases with diffuse histopathological characteristics with specific clinical profiles. Proper patient management begins with a precise diagnosis. Diagnosis should be based on a lymph node biopsy. The most common varieties in the pediatric population are Burkitt (40%), lymphoblastic lymphoma (30%), large B-cell diffuse lymphoma (20%) and 10% anaplastic lymphoma (10%). Initial approach of non-Hodgkin's lymphoma includes (spell out all abbreviations at first use: BH, EGO, ES, PFH, PFR, LDH), AMO, CSF and a chest X-ray and CAT. After defining whether the primary tumor is in the mediastinum, abdomen or head/neck, other studies can be considered such as magnetic resonance and positron emission tomography.[13] Initial approach with percutaneous renal biopsy, AMO and CSF was appropriate because the patient presented two oncological urgencies as well hemodynamic instability, requiring an urgent diagnosis. However, we must keep in mind the small amount of tissue makes diagnosis difficult. Broad-spectrum chemotherapy was started with a steroid and an alkylating agent. The steroid was essential at the beginning because a medullary infiltration was possible secondary to profound symmetrical weakness of lower limbs, probably absent tendinous reflexes, Babinsky response, rapid progression and no sphincter affection. Medullary compression syndrome should be quickly recognized in a pediatric cancer patient because children have the possibility to recover 100% of their functions with opportune treatment. This is common in lymphomatous leukemias. A neurological exam with the aforementioned elements may help to locate compression. Emergency therapy is administration of dexamethasone. Currently, laminectomy provided by neurosurgical services may be also considered. After 7 days of treatment, the myelosuppressive effect from chemotherapy can be appreciated in laboratory tests performed on July 9. The elevation of LDH is a consequence of large tumor destruction. Afterwards, the patient was managed with microtubule inhibitor and anthracycline. Differential diagnosis for this B-cell lymphoma should include:

1) A Burkitt non-Hodgkin's lymphoma from clinical presentation; abdominal lymphoma is the most common site of onset for non-Hodgkin's lymphoma in Mexico and renal infiltration is common.
2) A B-cell lymphoblastic lymphoma with a most unusual presentation because 85% of these lymphomas are associated with T-cells; abdominal presentation is infrequent because tumors are generally thoracic.
3) B-cell lymphoblastic leukemia with lymphomatous involvement is possible although we do not

have an AMO; we have to consider medullary cavity infiltration.

Infectious complications

This patient had the following risk factors: quantitative neutrophilic alterations at disease onset with reduced chemotaxis, antibacterial activity and superoxide radical production. As a result of nephrosis, she presented loss of immunoglobulins and alterations in B- and T-cell functions. Also, when beginning chemotherapy a generalized myelosuppression takes place, and leukocyte migration, phagocytic effect and opsonization processes are reduced. At the beginning of her disease, the patient was exposed to outside infections. Afterwards, vascular accesses and abdominal catheter were portals to other infections. Once chemotherapy was started, with natural barriers broken, internal flora play a predominant role. Initially the patient was managed with third-generation cefalosporin and a glycopeptides. The first septic shock occurred on July 9 manifested by a heat shock managed with crystalloids and norepinephrine. During this shock the patient presented the first cardiorespiratory arrest that required advanced maneuvers. A fourth-generation cephalosporin and an aminoglycoside were administered because of a catheter-related infection. Also, a broad-spectrum antibiotic for gram-positive bacteria sensitive to methicillin, enterobacteria and pseudomona was used. The first yeast identification was carried out with positive latex agglutination tests for *Candida*, adding amphotericin for management. When positive immunofluorescence was found for *Pneumocystis jirovecii*, treatment with trimethoprim-sulfamethoxazole was started. *C. tropicalis* was isolated. Our institution has a myriad of publications regarding fungal infections. In 1997 Pacheco et al. determined the associated mortality for pediatric patients hospitalized who presented systemic candidiasis and found a mortality rate of 46.5% in 71 cases during a 2-year study.[14] The most important finding was that mortality increased significantly each day that the treatment was delayed with a 1.12 odds ratio. Guzman reported an increment in the frequency of infections from non-albicans *Candida* spp. in the neonatal ICU (NICU) in 52% of cases.[15] This situation has been reported worldwide. An article in the journal *Pediatrics* analyzed the molecular characterization and antimicrobial susceptibility in pediatric and neonatal patients in Australia during a 4-year period with 1 005 cases. Of these cases, 33 were presented in newborns, 110 in children and 862 in adults. Significant risk factors in children include neutropenia, hematological cancer, renal or urological disease and hemodalysis, all presented by our patient.[16] An in-process study at the Department of Infectology that included 96 patients found that 53% presented candidemia and 46% disseminated candidiasis. Species found include *C. albicans* (51%), *C. tropicalis* (27%), *C. parapsilosis* (10%) and *C. glabrata* (7%). Of the cases, 25% were found in patients with leukemia or lymphoma. Despite the fact that the international literature describes 75% therapeutic failure using amphotericin on several *Candida* spp. with minimal inhibitory concentrations ($>1\ \mu$g/dL), this has not been corroborated in our hospital. It has also not been established that *Candida* spp. sensitivity depends on dosage. Antifungal drug change was appropriate because of a lower toxicity profile as demonstrated in a controlled clinical trial carried out in Chicago and included 82 children, finding similar favorable evolution rates (46.4% for caspofungin and 32% for amphotericin-B) with milder adverse effects in the caspofungin group (1.2 *vs* 11.5%).[17] Afterwards, because of a continued systemic inflammatory response with severe neutropenia, the empirical schema was modified to include resistant gram-negative bacteria with carbapenem. We found images compatible with microabscesses in the kidney and a suspected endocarditis. The latest therapeutic resources included gammaglobulin to promote passive immunity and increase antibody titers as well as antibody antigen reaction potential. Sepsis progressed to multiorgan dysfunction syndrome as follows: progressive cardiovascular dysfunction requiring volume and vasoactive amines

attempting to increase contractility and chronotropism, increasing peripheral vascular resistance with an integrated pump as reflected by ejection fraction 1 day before the patient's death with a distributive pattern that could not be controlled because of severe immunosuppression. Ventilatory dysfunction evolved from acute pulmonary damage to acute respiratory distress syndrome (ARDS) with progressive deterioration of oxygenation indices that did not respond to usual alveolar recruitment maneuvers. Finally, the patient required high-frequency oscillatory ventilation. As observed in X-rays, lung images may have multiple etiologies (infection, disease progression, drug reactions, embolism and hemorrhages). There was hematological dysfunction with pancytopenia and consumption coagulopathy. Renal dysfunction stabilized during the last days without metabolic criteria for dialysis, which can be considered as an improvement in ARI onset from the beginning. Final diagnoses are as follows:

- Eutrophic female child
- Epstein-Barr virus infection
- Possible lymphoid neoplasms: Burkitt's lymphoma stage III vs. B-cell lymphoblastic lymphoma stage III vs. acute B-cells lymphoblastic leukemia TLS
- Medullary compression syndrome
- Nephrotic syndrome secondary to infiltration
- ARI
- Catheter-related infection
- Severe disseminated candidiasis
- Ventilator-associated late nosocomial pneumonia
- Septic shock
- Multiorgan dysfunction syndrome with cardiovascular, respiratory, hematological and renal dysfunction

Pathology findings

Dr. Stanislaw Sadowinski Pine

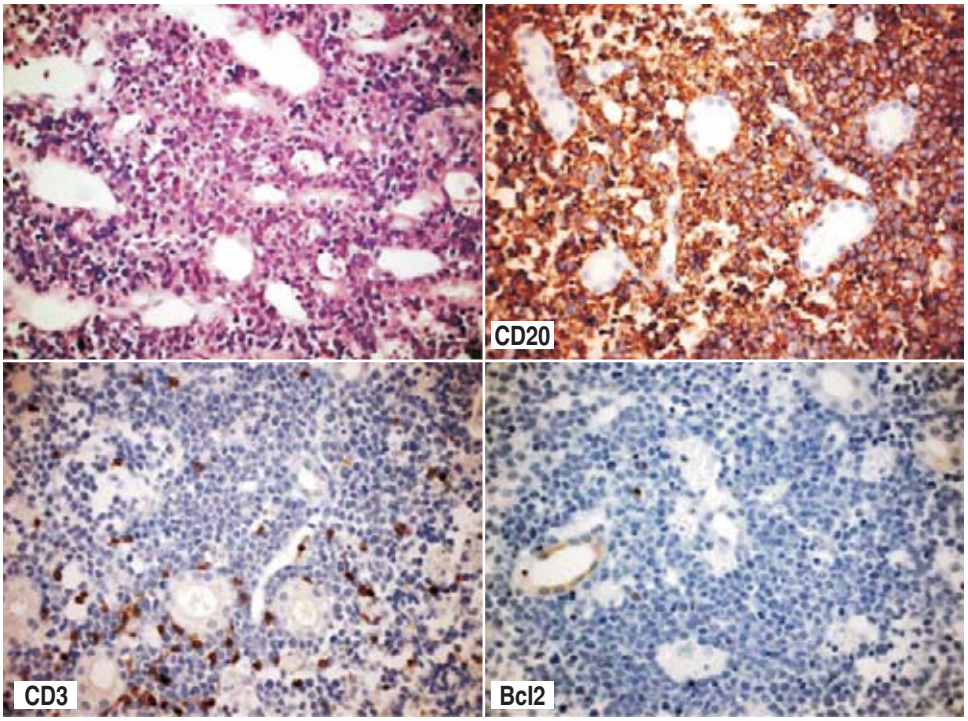

Figure 6. (a) Renal parenchyma with diffuse infiltration from lymphoid cells (H/E x 400). (b) CD20 cytoplasmic expression with membrane pattern. (c,d) Neoplastic cells negative for CD3 and Bcl2 (immunohistochemistry x 400).

The first contact with this patient in the Department of Pathology was through a puncture renal biopsy that showed diffuse infiltration at interstitium by small round cells that presented a discreet star sky pattern of phagocyting cell detritus with some parts showing epithelial cells from renal tubules. From immunohistochemical analysis, cells were positive for CD19 and CD20 and negative for CD3, Bcl2 and Tdt, corresponding to a non-Hodgkin's lymphoma with a pattern compatible with Burkitt's lymphoma. Cells that express CD20 represent most of the cells that infiltrate renal parenchyma and we also observe some CD3+ T-cells (Fig. 6). A bone marrow biopsy was also received showing reduced population (20% cellularity) having precursors from megakaryocytic, granulocytic and erythroid series without infiltration from lymphoma cells.

At autopsy we observed enlarged kidneys: right kidney (250 g), left kidney (308 g) (expected weight 90 g). The section showed poor differentiation between cortex and medulla and multiple whitish-yellow calcifications without abscesses. Upon microscopic analysis we can observe the large number of calcifications and necrosis of 90% neoplastic cells, chiefly in the cortex. Glomerulus presented no changes and there were some inflammatory cells in the interstice. Immunohistochemistry revealed viability in ~10% of lymphoma cells expressing CD20. Necrosis from lymphoma cells can be observed in other areas after chemotherapy, and we precipitated DNA in basal membrane of tubules and walls of some capillary vessels. This phenomenon was described originally in carcinomas of pulmonary small cells in adults, and it is known as Azzopardi phenomenon (Fig. 7). Other changes are acute tubular necrosis and hypokalemic nephropathy.

Brain presents atrophy with lateral ventricular dilation. Subarachnoid space showed infiltration by lymphoma cells expressing CD19 and CD20 (Fig. 8), being the largest tumor viability site. Lymphoma was disseminated to digestive tube and left ovary where we observed neoplastic cells and extensive areas of calcification.

The liver weighed two times as much as we expected, having discreet vascular congestion and sinusoidal dilation. The spleen also had an increased

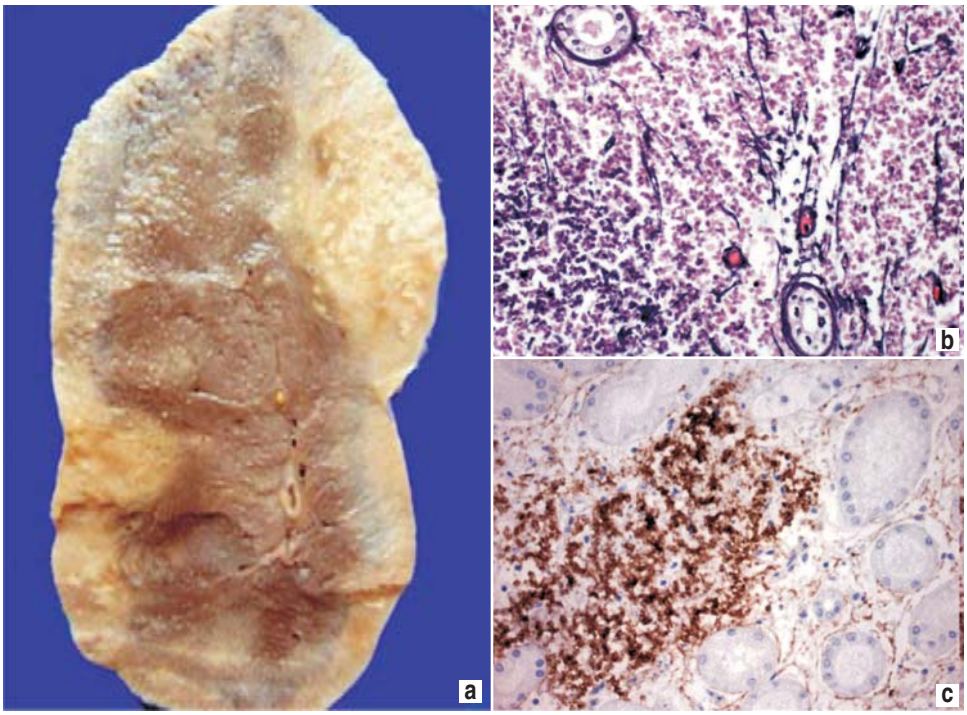

Figure 7. (a) Kidney section. Note multiple calcifications at cortex and medulla. (b) Coagulative necrosis of neoplastic cells and calcification on vascular walls and tubules (H/E ´400). (c) CD19-positive groups of neoplastic cells (immunohistochemistry x 400).

size due to congestion and both organs presented no lymphoma infiltration.

Lungs presented parenchymal consolidation and a smooth aspect with yellowish areas alternating with dark areas forming nodules (Fig. 9). Histologically there are mucus plugs in the bronchi and bronchioli, and no free air is observed. Alveolar walls showed a yellowish color on H/E stain and von Kossa stain. These areas match calcifications that cause rupture of alveolar capillaries, hemorrhages, organization and fibrosis. This calcification is observed not only in alveolar walls but also in basal membrane from terminal and respiratory bronchioli as well as artery wall.

Other lung sections reveal diffuse lung damage with hyaline membranes and pneumocytes with numerous viral inclusions (intranuclear and cytoplasmic) from cytomegalovirus (CMV) and bronchiolitis obliterans with polypoid structures affecting bronchioli, alveolar ducts and sacs (Fig. 10). None of the sections revealed mycotic infection or lymphoma infiltration.

Clinical history mentions endocarditis. Heart is enlarged; however, we found no vegetation in any cardiac cavity. On the left atrium wall we observed confluent yellowish plaques that match calcification affecting even the coronary artery (Fig. 11).

Parathyroid glands weighed 300 g (expected weight 60 g). They changed their elongated shape to a nodular shape and showed increase of main cells and absence of adipocytes (Fig. 12).

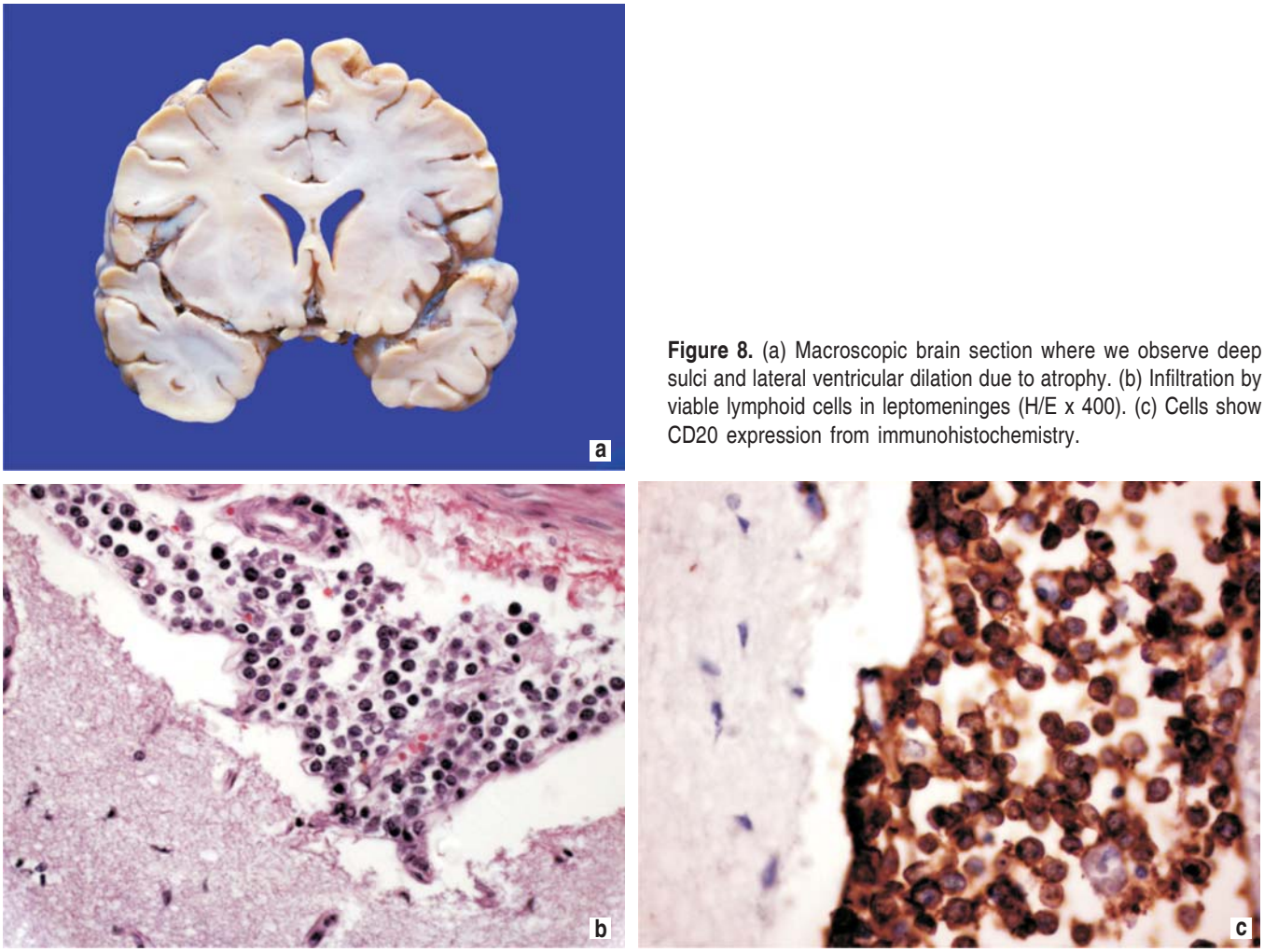

Figure 8. (a) Macroscopic brain section where we observe deep sulci and lateral ventricular dilation due to atrophy. (b) Infiltration by viable lymphoid cells in leptomeninges (H/E x 400). (c) Cells show CD20 expression from immunohistochemistry.

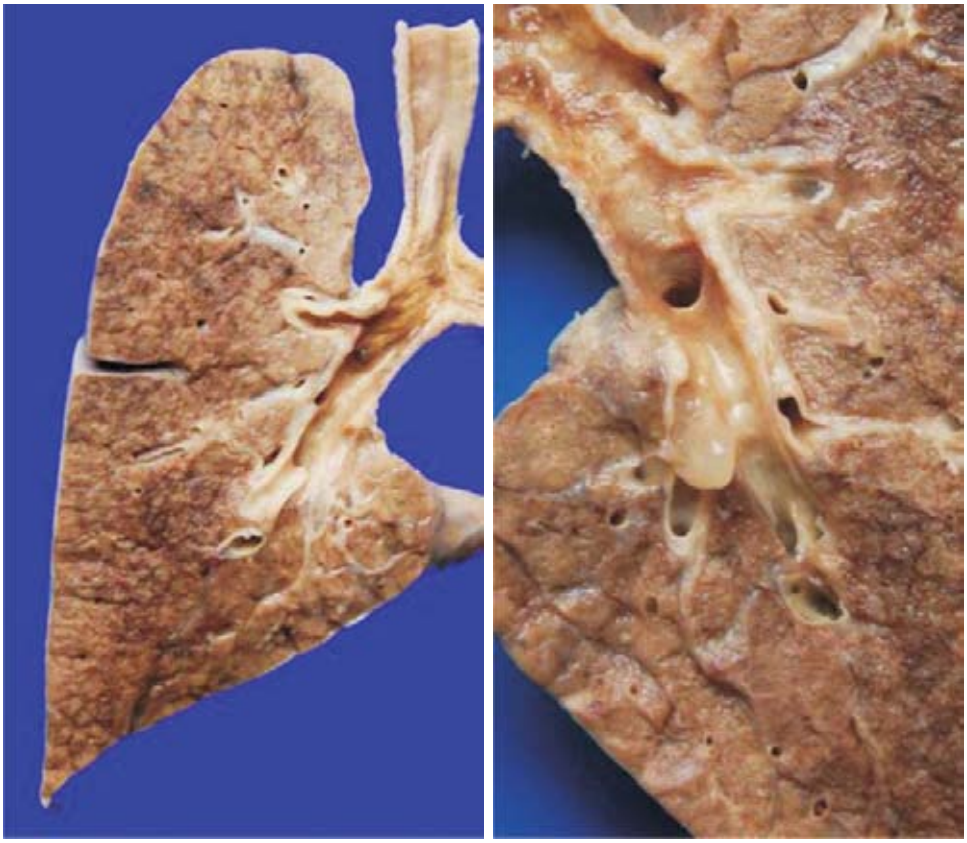

Figure 9. Lung section with consolidation and smooth aspect of parenchyma and mucus plugs in bronchi.

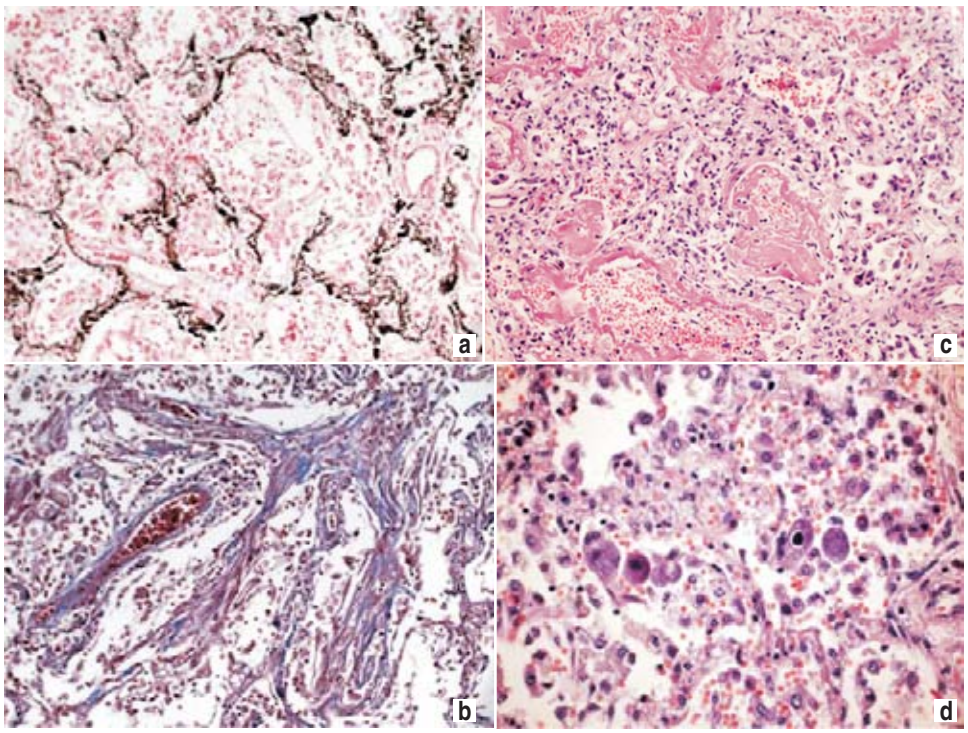

Figure 10. (a) Calcified alveolar walls (von Kossa stain x 400). (b) Hyaline membranes in alveolar sacs and ducts and recent intra-alveolar hemorrhage (H/E x 400). (c) Microphotography showing polypoid structures organized in alveolar sacs and ducts (Masson's trichrome stain x 400). (d) Pneumocytes with intranuclear inclusions from CMV (H/E x 400).

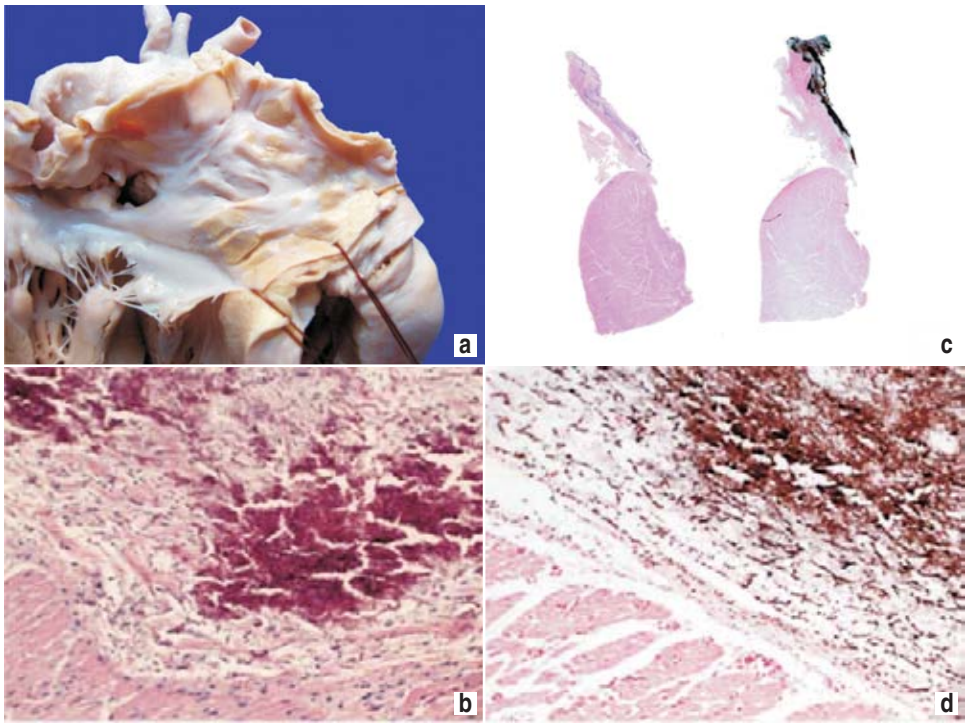

Figure 11. (a) Internal surface from left auricle with yellowish calcified plaques. (b) Section of atrium and left ventricle with atrial wall calcification (von Kossa stain). (c) Myocardium with metastatic calcification (H/E x 400). (d) Calcium deposit stains in black (von Kossa x 400).

This patient also presented pancreatitis from CMV. We observed a large number of viral inclusions with mononuclear-type inflammatory infiltration.

In the spinal cord we found normal anterior horn neurons without demyelination of spinal nerve roots. These findings discard polyradiculopathy secondary to azotemia described in the clinical history. We also found atrophic thymus with almost complete absence of T-cell lymphocytes and calcified Hassall's corpuscles, some being dilated.

Bone marrow presented no infiltration from lymphoma. The sample was taken from bones of vertebral bodies and costal and iliac crest. Histopathological diagnoses are as follows:

- Burkitt's lymphoma with infiltration to kidneys, left ovary, small intestine, colon and leptomeninges
- Necrosis of 90% neoplastic cells secondary to chemotherapy, with dystrophic calcification
- Bilateral nephromegaly
- Secondary hyperparathyroidism with hyperplasia of parathyroid glands; metastatic calcifications in alveolar partitions, bronchi, bronchioli, pulmonary vessels, left atrium of the heart and coronary arteries
- Acute pulmonary damage characterized by diffuse alveolar damage and bronchiolitis obliterans
- CMV infection in lungs and pancreas
- Hemaphagocytic syndrome due to CMV infection
- Cardiomegaly
- Thymus atrophy
- Brain atrophy with ventricular dilation
- Tubular necrosis
- Bilateral hydrothorax
- *Postmortem* cultures positive for *Enterococcus* sp. in blood and *E. faecium* in small intestine and colon
- Negative CSF, lung, spleen and liver

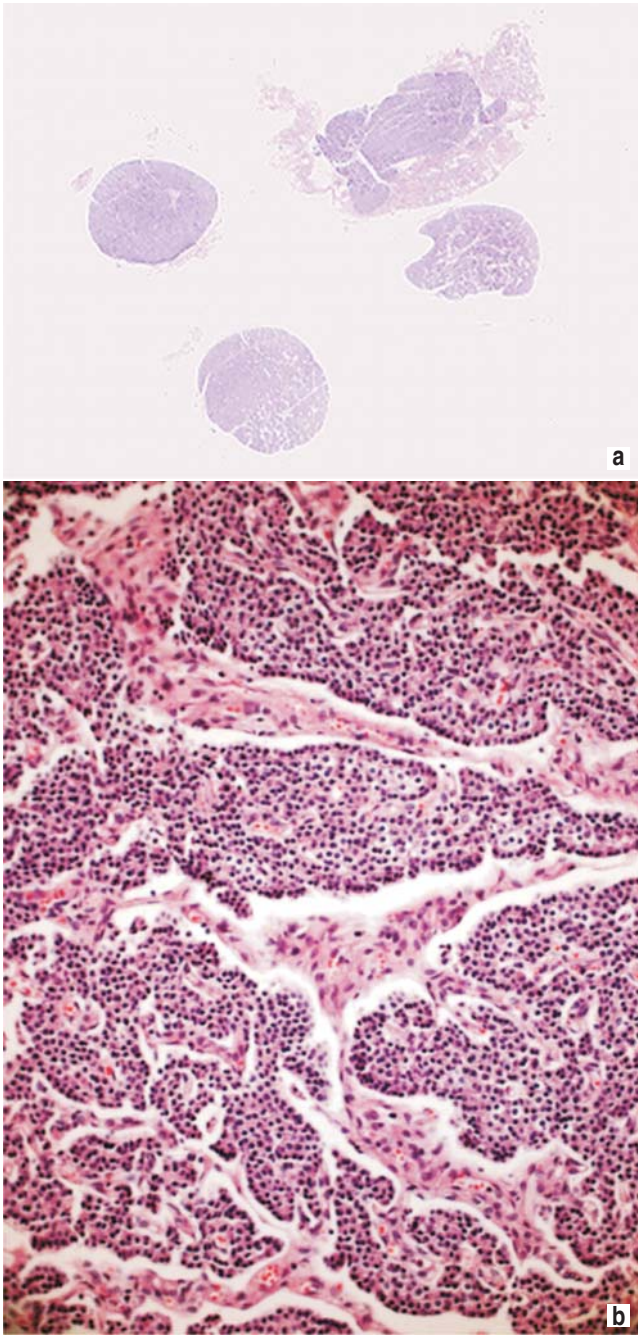

Figure 12. (a) Parathyroid microphotography showing all are increased in size (H/E). (b) Histology from one gland with hyperplasia of main cells and absence of adipocytes (H/E x250).

Oncological urgency comments

Dr. Rebeca Gomezchico Velasco

Patients with lymphoma present various renal alterations. This patient, considering the rapid development of Burkitt's lymphoma, possibly presented previous TLS, which caused the renal insufficiency at admission. We should use utmost care with clinical data because a thorough physical examination would have revealed enlarged kidneys. Kidney damage without accelerating cause should be evaluated with other tests, even renal ultrasound. Renal alterations in a general urinalysis can manifest as leukocyturia, proteinuria, presence of casts, etc. Other manifestations of renal alteration are anuria secondary to compression from lymphoma and renal artery/vein thrombosis.

Incidence of renal alterations in patients with Burkitt's lymphoma is unknown although it has been estimated that 50% of cases present evident or hidden manifestations. The patient presented here had onset of renal insufficiency and, therefore, dialysis was indicated. This is highly recommended to limit damages secondary to TLS that usually complicates these cases.

Dr. José Loeza Olive

It is important to highlight that recently diagnosed oncology patients can present with one or many oncological urgencies. Our patient presented TLS and medullary compression. Tumor lysis is presented in patients with rapidly growing tumors such as Burkitt's lymphoma and T-cell lymphoblastic leukemia. As for medullary compression syndrome, this is frequently associated with lymphoma, Ewing's sarcoma, rhabdomyosarcoma and osteosarcoma. It is important to recognize and identify these urgencies in a timely manner so that treatment is able to improve diagnosis. It is possible that our patient presented radicular pain before presenting walking difficulty at admission. This discards medullary compression and requires imaging studies such as magnetic resonance, as well as initiation of steroid treatment.

The patient arrived with peritoneal dialysis at admission. It is possible the patient presented hyperphosphatemia, hyperkalemia and hyperuricemia that were not opportunely identified. It is important to highlight that TLS treatment is prophylactic with

hyperhydration, urinary alkalization and management of metabolic alterations.

In our case, the patient died even though neoplastic recovery is >90%. Therefore, this stresses the importance of establishing prophylactic and therapeutic treatment for oncological urgencies.

Correspondence to:
Dr. Luis Enrique Juárez Villegas
Hospital Infantil de México Federico Gómez
México, D.F., México
E-mail: luisjuarez13@hotmail.com

References

1. Ignacio Zaragoza, Durango. Available at: http://mexico.pueblosamerica.com/i/ignacio-zaragoza-23/
2. Belson M, Kingsley B, Holmes A. Risk factors for acute leukemia in children: a review. Environ Health Perspect 2007;115:138-145.
3. Reardon JZ. Environmental tobacco smoke: respiratory and other health effects. Clin Chest Med 2007;28:559–573.
4. Buka I, Koranteng S, Osornio-Vargas AR. Trends in childhood cancer incidence: review of environmental linkages. Pediatr Clin North Am 2007;54:177-203.
5. Flower KB, Hoppin JA, Lynch CF, Blair A, Knott C, Shore DL, et al. Cancer risk and parental pesticide application in children of Agricultural Health Study participants. Environ Health Perspect 2004;112:631-635.
6. Ma X, Buffler PA, Gunier RB, Dahl G, Smith MT, Reinier K, et al. Critical windows of exposure to household pesticides and risk of childhood leukemia. Environ Health Perspect 2002;110:955-960.
7. Rezk S, Weiss L. Epstein-Barr virus-associated lymphoproliferative disorders. Hum Pathol 2007;38:1293-1304.
8. Gordillo R, Spitzer A. The nephrotic syndrome. Pediatr Rev 2009;30;94-105.
9. Olowu WA, Adelusola KA. Pediatric acute renal failure in southwestern Nigeria. Kidney Int 2004;66:1541–1548.
10. Coiffier B, Altman A, Pui C, Younes A, Cairo M. Guidelines for the management of pediatric and adult tumor lysis syndrome: an evidence-based review. J Clin Oncol 2008;26:2767-2778.
11. Mukherjee E, Mukherji D, Jayawardene SA, Kon SP. Tumor lysis syndrome and acute renal failure: an increasing spectrum of presentations. Clin Nephrol 2007;68: 186-189.
12. Good DJ, Gascoyne RD. Classification of non-Hodgkin's lymphoma. Hematol Oncol Clin North Am 2008;22:781-805.
13. Matasar M, Zelenetz A. Overview of lymphoma diagnosis and management. Radiol Clin North Am 2008;46:175-198.
14. Pacheco RA, Ávila FC, Nobigrot KD, Santos JI. Mortality associated with systemic candidiasis in children. Arch Med Res 1997;28:229–232.
15. Guzmán B. Frecuencia de especies y patrón de susceptibilidades de *Candida* spp. aisaldas de sitios estériles en pacientes de una unidad de cuidados intensivos neonatales en un periodo de cuatro años. Tesis para obtener el título de Infectología Pediátrica. Hospital Infantil de México; 2008.
16. Blyth CC, Chen SC, Slavin MA, Serena C, Nguyen Q, Mariott D, et al. Not just little adults: candidemia epidemiology, molecular characterization, and antifungal susceptibility in neonatal and pediatric patients. Pediatrics 2009;123:1360-1368.
17. Maertens J, Madero L, Reilly A, Lehrnbecher T, Groll A, Jafri H, et al. A randomized, double blind, multicenter trial of caspofungin (CAS) *versus* liposomal amphotericin B (LAMB) for empirical antifungal therapy (EAFRx) of pediatric patients with persistent fever and neutropenia (PFN). In: Abstracts of the 47th Interscience Conference on Antimicrobial Agents and Chemotherapy. American Society of Microbiology, Washington DC; 2007: Abstr. M-621, p. 435.